Accepted Manuscript

International Journal of Wavelets, Multiresolution and Information Processing

World Scientific
www.worldscientific.com

Accepted manuscript to appear in IJWMIP

October 20, 2017   8:58   WSPC/WS-IJWMIP   ws-ijwmip

A Novel Fast Detection Method of Infrared LSS-Target in Complex Urban Background

Yanfeng Wu[†,‡], Haijiang Sun[*,†] and Peixun Liu[†]

*Fast Capture and Real-time Image Processing Technology Lab, Changchun Institute of Optics,
Fine Mechanics and Physics, Chinese Academy of Sciences,
Changchun, 130033, P. R. China[†]*

*University of Chinese Academy of Sciences
Beijing, 100049, P. R. China[‡]
wuyfciomp@yahoo.com
sunhaijiang@126.com
liupeixun@126.com*

LSS-Target (the Low altitude, Slow speed and Small Target) is likely to be a threat
to the observation platform, thus infrared LSS-Target detection is an urgent task. LSS-
Target is a challenging issue due to the low Signal-to-Noise Ratio (SNR) and sophis-
ticated background. Motivated by the analysis of infrared imaging characteristics, this
paper proposes a novel fusion method for IR LSS-Target detection with complex urban
background, which is suitable for precise guidance and self defense. Firstly, an adap-
tive threshold segmentation based on accumulative histogram and maximum likelihood
estimation are utilized to eliminate the clutter and improve SNR of the initial image.
Secondly, a template is set up to identify the seed points in the image. Thirdly, a con-
strained four criteria region growth algorithm is performed to separate the entire regions.
Finally, the confidence measure is constructed, which can eliminate false targets and the
background edges. Experimental results show that the method in this paper can screen
out the real LSS-Target in real time with high accuracy under sophisticated background.

Keywords: Adaptive threshold segmentation; region growth; small target detection.

AMS Subject Classification: 22E46, 53C35, 57S20

1. Introduction

LSS-Target (the Low altitude, Slow speed and Small Target) is an aircraft or a
floating object at a flight height lower than 2000 meters and a speed less than
200km/h. As representatives, small aircraft, UAVS and aviation models develop

---

*Corresponding author

2 *Yanfeng Wu,Haijiang Sun and Peixun Liu*

fast in recent years. LSS-Target detection is widely used in searching, tracking and surveillance systems, consequently it is very important and urgent to detect the LSS-Target effectively in real time.

Many algorithms related to LSS-Target detection have been put forward in recent years, which can be grossly classified into two groups: single frame detection and sequential frames detection. Single frame detection finds targets without interframe prediction and compensation, which is of great concern in defense system. Yu et al. designed a Gaussian kernel to suppress the random noise and performed the region growth to filter out the large regions.[1] Fan et al. used morphology operators and correlation filter to extract characteristic vectors of small target.[2] Besides, particle filter,[3] median filter,[4] matched filter,[5] wavelet transformation[6] and Partial Differential Equation (PDE)[7,8] are commonly used in single frame detection. These algorithms can remove noises and enhance the contrast of image. However, they are not applicable to the complex urban area.

Sequential frames detection requires prior information and is able to process images with more complex background. Visual Background Extractor (ViBe) described by Olivier Barnich and Marc Van Droogenbroeck is able to detect the LSS-Target in a static scene. ViBe can be initialized with a single frame, which is free of pause for the subsequent detection.[9] Nieet al. proposed a method, which models background after analyzing the image properties and detect the moving dim targets by Multi-level Hypothesis Testing (MHT).[10] Y. Zhang et al. proposed a method based on Three-Fame Difference, which can perform real-time detection but with high false alarm rate.[11] E. Guariglia analysed the entropies of Shannon, Rnyi and Kolmogorov[13] as well as Weierstrass-Mandelbrot Function[14] and computed fractional derivative of the Riemann zeta function, which is applicable and effective in IR image processing.[15,16]

In order to detect LSS-targets under dynamic and homogeneous background in real time, a novel fusion detection method with high accuracy is proposed in this paper. Firstly, adaptive threshold segmentation based on accumulative histogram and maximum likelihood estimate are used to eliminate the clutter and improve the SNR. Secondly, a template is set up to identify the seed point in the image. Thirdly, a constrained four criteria region growth algorithm is performed to separate regions. Finally, a small round target filter is constructed, which can eliminate false target and the background edges. Experimental results show that the performance of our method is better than Visual Background Extractor and Three Frame Difference method.

This paper includes the following structure and main contents: the first part is an introduction of the current research status. In the second chapter, we analyze the features of LSS-Target. In the third chapter, a detailed description about our method is given. The experimental results are provided in the fourth chapter. Finally, we summarize the article in the last section.

2. Features of LSS-Target

Due to the effects of atmospheric thermal noise, long distance transmission and noise of detection devices, LSS-Target usually exhibits the following three characteristics:

- The target spans a few pixels in the image, and the shape is similar to the point target;
- The SNR of the image under the remote camera is not high, and the target is usually hidden in the background;
- There are complex background such as buildings, woods and white cloud, which is conducive to ineffective detection of target.

The difficulties of small target detection are as follows:

- The lack of prior information of the background;
- Low SNR of the image makes it not easy to distinguish the background, the targets and the noises;
- The target may disappear from the background intermittently, which is difficult to predict;
- The lack of shape and texture features.

The infrared characteristics of LSS-Target are mainly the radiation caused by aerodynamic heating. When the target is moving, the surface of the target is heated by friction with the air, and the temperature of the target surface T_s can be calculated as follows:

$$T_s = T_0(1 + 0.16M^2) \tag{2.1}$$

where T_0 is the atmospheric temperature, and M is the Mach number, which is corresponding to the target velocity.

The Plank blackbody radiation law reveals the law of the black body radiation energy in terms of wavelength and temperature, and its mathematical expressions are as follows:

$$W_B(\lambda, T) = \frac{c_1}{\lambda^5} \cdot \frac{1}{(e^{c_2/\lambda T} - 1)} \tag{2.2}$$

$$I_B(\lambda, T) = \frac{c_1}{\pi\lambda^5} \cdot \frac{1}{(e^{c_2/\lambda T} - 1)} = \frac{W_B(\lambda, T)}{\pi} \tag{2.3}$$

where $W_B(\lambda, T)$ is the blackbody spectral irradiance, λ is the wavelength, T is the thermodynamic temperature of the blackbody radiation, the first radiation constant $c_1 = 3.742 \times 10^6 W \cdot m^{-2}$, the second radiation constant $c_2 = 1.4388 \times 10^{-2} W \cdot K$, $I_B(\lambda, T)$ is the spectral emissivity of the blackbody, which is the intensity of radiation emitted per unit area, unit time, and unit wavelength.

Assuming that the ambient temperature is $10°C$ and the target flight velocity is $0\text{-}2.5Ma$, the spectral spectrum can be calculated by the formula Eq. (2.1), Eq.

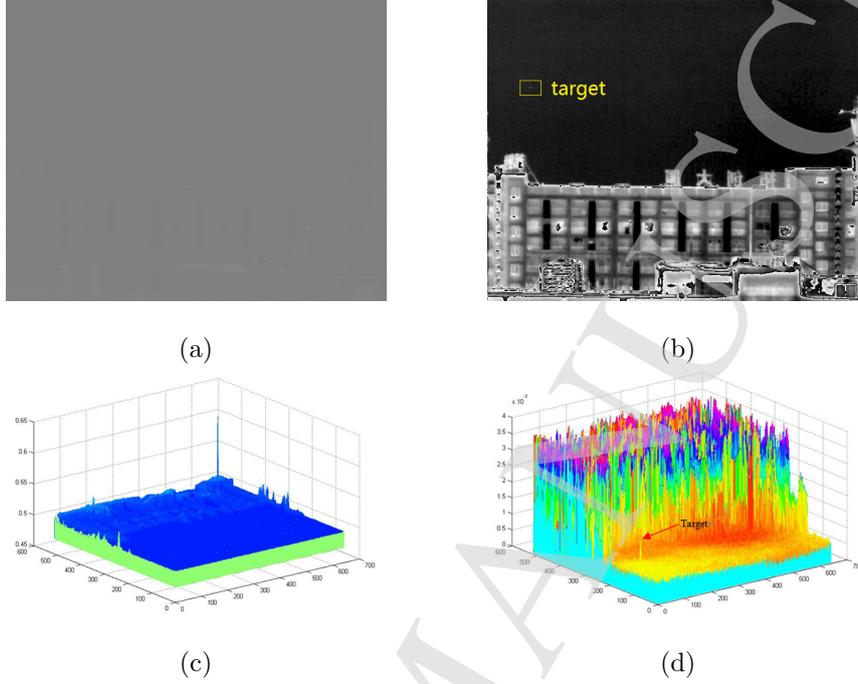4   *Yanfeng Wu,Haijiang Sun and Peixun Liu*

(a)

(b)

(c)

(d)

Fig. 1. Features of LSS-Target. (a) Original IR image. (b) Stretched image. (c) 3D-mesh view of the original image. (d) 3D-mesh view of the stretched image.

(2.2), Eq. (2.3) and the peak wavelength is $6 - 10\mu m$.The peak wavelength of sky background brightness during the day time is from 3 to 5 μm, and peak wavelength of sky background at night from 8 to 12 μm. So the temperature difference between background and target is relatively small, the gray value of the infrared image is low and concentrated. The energy distribution is shown in Fig. 1.a. A general IR image is modeled as Eq. (2.4)[12]

$$F(x,y) = T(x,y) + B(x,y) + N(x,y) \tag{2.4}$$

where $T(x,y)$ represents the target,$B(x,y)$ and $N(x,y)$ represent the background clutter and the noise respectively.

The original image is a 16-bit gray scale image with a low contrast. It is quite impossible to find the target from the original image. In order to analyze the characteristic of the LSS-Target in the image, it is necessary to stretch 16-bit image into 8-bit image, and the formula is as follows:

$$s = T(r) \tag{2.5}$$

$$T(r) = \frac{255 \times (r - min)}{(max - min)} \tag{2.6}$$

A Novel Fast Detection Method of Infrared LSS-Target in Complex Urban Background   5

where r is the gray value before transformation, and s is the gray value after transformation. Max is the maximum gray level in the image, and min is the minimum. The result is shown in Fig. 1.b.

From the results, it can be concluded that the gray values of the sky background and the urban area could be considered well-distributed, and the gray value of the urban area is larger than that of the sky background. What's more, the gray value of LSS-Target is between urban background and sky background.

3. Detection Algorithm

First of all, this paper uses double Gauss function to fit statistic histogram. Maximum likelihood estimation (MLE) is presented and used to calculate the threshold value and to extract the region of interest (ROI). Secondly, Local maxima method is proposed to find pixels that belong to possible LSS-Target. Next, we perform the constrained four criteria region growth to filter out the large areas of clutter. Finally, we construct the confidence measure to screen out the real target from the candidate targets. Fig. 2 is the flow chart of proposed method.
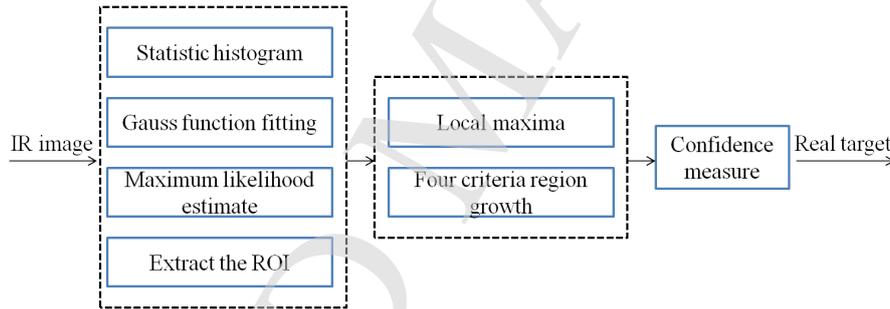

Fig. 2. Flow chart of proposed detection method.

3.1. *The Choice of ROI based on MLE and Histogram Statistic*

Under normal conditions, image with complex background always has different intensity distributions. Thus, to find the target, an effective and adaptive division method is needed.

The cumulative histogram represents the cumulative probability distribution of the image components at the gray level. Each value represents the probability of being less than or equal to the gray value. Consider the cumulative images histogram is a discrete function and the gray level is from 1 to L-1:

$$H(s_k) = n(k) \qquad k = 0, 1, \cdots, L-1 \tag{3.1}$$

6   *Yanfeng Wu,Haijiang Sun and Peixun Liu*

$$P(s_k) = \frac{H(s_k)}{n} \qquad k = 0, 1, \cdots, L-1 \tag{3.2}$$

where n is the total pixels of the image and s_k is the value of gray level k. $n(k)$ is total pixels of s_k and $P(s_k)$ is the occurrence probability estimation of the gray level s_k.
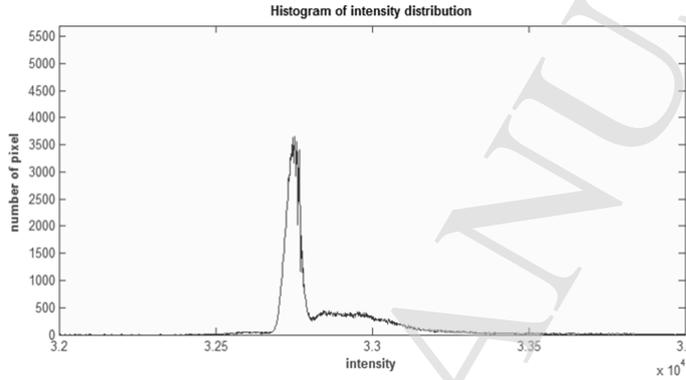

Fig. 3. Histogram of original IR image.

Normally, for the images with many targets and a complex background has a multi-modal histogram. Histograms can be viewed as a superposition of multi-Gaussian distributions, for decomposition of multi-Gaussian can fit the multi-modal characteristics of histogram. The histogram of the original IR image is shown in Fig .3. In this paper, double Gauss function is used to fit the histogram.

$$f(x) = a_1 \cdot exp[-(\frac{x - b_1}{c_1})^2] + a_2 \cdot exp[-(\frac{x - b_2}{c_2})^2] \tag{3.3}$$

Where a_1, b_1, c_1, a_2, b_2 and c_2 are undetermined parameters. Maximum likelihood estimate (MLE) is firstly proposed by C. F. Gauss in 1922, which can compute the probability density of the discrete random variables. In this paper, MLE is used to compute the unknown parameter of double Gauss function. Likelihood function L is as follows:

$$L(a_1, b_1, c_1, a_2, b_2, c_2) = \prod_{k=1}^{n} \{a_1 \cdot exp[-(\frac{n_k - b_1}{c_1})^2] + a_2 \cdot exp[-(\frac{n_k - b_2}{c_2})^2]\} \tag{3.4}$$

Taking logarithm

$$\ln L(a_1, b_1, c_1, a_2, b_2, c_2) = \sum_{k=1}^{n} \{\ln a_1 \cdot exp[-(\frac{n_k - b_1}{c_1})^2] + a_2 \cdot exp[-(\frac{n_k - b_2}{c_2})^2]\} \tag{3.5}$$

A Novel Fast Detection Method of Infrared LSS-Target in Complex Urban Background 7

Solve the partial derivative of $\ln L$ with respect to a_1, b_1, c_1, a_2, b_2 and c_2, make them equal to zero, then we get:

$$
\begin{cases}
\dfrac{\partial L(a_1,b_1,c_1,a_2,b_2,c_2)}{\partial a_1} = \sum_{k=1}^{n}\left\{\dfrac{1}{a_1 + a_2 \cdot exp[(\frac{n_k-b_1}{c_1})^2 - (\frac{n_k-b_2}{c_2})^2]}\right\} = 0 \\[4mm]
\dfrac{\partial L(a_1,b_1,c_1,a_2,b_2,c_2)}{\partial b_1} = \sum_{k=1}^{n}\left\{\dfrac{\frac{2n_k}{c_1{}^2} - \frac{2b_1}{c_1}}{1 + \frac{a_2}{a_1} \cdot exp[(\frac{n_k-b_1}{c_1})^2 - (\frac{n_k-b_2}{c_2})^2]}\right\} = 0 \\[4mm]
\dfrac{\partial L(a_1,b_1,c_1,a_2,b_2,c_2)}{\partial c_1} = \sum_{k=1}^{n}\left\langle\dfrac{2(n_k-b_2)^2}{c_1{}^3 \cdot \{1 + \frac{a_2}{a_1} \cdot exp[(\frac{n_k-b_1}{c_1})^2 - (\frac{n_k-b_2}{c_2})^2]\}}\right\rangle = 0
\end{cases}
\tag{3.6}
$$

$$
\begin{cases}
\dfrac{\partial L(a_1,b_1,c_1,a_2,b_2,c_2)}{\partial a_2} = \sum_{k=1}^{n}\left\{\dfrac{1}{a_1 \cdot exp[(\frac{n_k-b_2}{c_2})^2 - (\frac{n_k-b_1}{c_1})^2] + a_2}\right\} = 0 \\[4mm]
\dfrac{\partial L(a_1,b_1,c_1,a_2,b_2,c_2)}{\partial b_2} = \sum_{k=1}^{n}\left\{\dfrac{\frac{2n_k}{c_2{}^2} - \frac{2b_2}{c_2}}{1 + \frac{a_1}{a_2} \cdot exp[(\frac{n_k-b_2}{c_2})^2 - (\frac{n_k-b_1}{c_1})^2]}\right\} = 0 \\[4mm]
\dfrac{\partial L(a_1,b_1,c_1,a_2,b_2,c_2)}{\partial c_2} = \sum_{k=1}^{n}\left\langle\dfrac{2(n_k-b_1)^2}{c_2{}^3 \cdot \{1 + \frac{a_1}{a_2} \cdot exp[(\frac{n_k-b_2}{c_2})^2 - (\frac{n_k-b_1}{c_1})^2]\}}\right\rangle = 0
\end{cases}
\tag{3.7}
$$

where a_1, b_1, c_1, a_2, b_2 and c_2 are the solutions of Eq. (3.1), Eq. (3.6) and Eq. (3.7). The fitting results of Fig. 3 are shown in Fig. 4. According to Eq. (3.8), Q, the trough of the double Gaussian function as well as the threshold to extract the ROI of the image, can be obtained. Eq. (3.9) is used to extract the ROI in the image.

$$
\begin{cases}
\dfrac{\partial L(x)}{\partial x}\Big|_{x=Q} = 0 \\[3mm]
\lim_{x \to Q^+} \dfrac{\partial L(x)}{\partial x} = 0 \\[3mm]
\lim_{x \to Q^-} \dfrac{\partial L(x)}{\partial x} = 0
\end{cases}
\tag{3.8}
$$

$$
g(x,y) = \begin{cases} f(x,y), & g(x,y) < Q \\ 0, & g(x,y) \geq Q \end{cases}
\tag{3.9}
$$

where $f(x,y)$ is the gray value of the original image at (x,y), and $g(x,y)$ is the image after the preprocess.

3.2. *Marking the seed points*

The local energy of LSS-Target is aggregated, so the gray value of the pixel at the target always exhibits local maxima characteristics in the neighboring region. Thus, it is useful to perform a local maxima detection to mark seed points which may belong to a possible target. The local maxima detection can be performed by a $T \times T$ averaging template. The current point whose gray value is considerably

8   *Yanfeng Wu,Haijiang Sun and Peixun Liu*

higher than the average gray value of the neighbors in the template is marked as local maxima. Given a gray image f, the gray value of seed point $p(x,y)$ is $f(x,y)$, then the local maxima image of g is calculated as following:

Algorithm 1 Local Maxima Algorithm

Step 1: setting $T \times T$ window to traverse the entire image, as shown in Fig. 5.The length of step is one.

Step 2: calculate the mean of pixels in the $T \times T$ window with Eq. (3.10):

$$median = \frac{1}{T \times T} \sum_{i=-1}^{1} \sum_{j=-1}^{1} f(i,j) \qquad (3.10)$$

Step 3: As shown in Eq. (3.11), comparing the difference between the mean values and the gray values of the pixels in the window. If the difference is beyond the threshold, then mark it as a seed point.

$$g(x,y) = \begin{cases} p(x,y), & if \ f(x,y) - meadian < \alpha \\ 0, & if \ f(x,y) - meadian \geq \alpha \end{cases} \qquad (3.11)$$

where α is a threshold to evaluate how salient the LSS-Target is, compared to the background in the neighborhood, which is 10 in our case. The width of window T is 3 in our case.Some of the local maxima belong to small targets, but others may belong to the edges of background, which should be eliminated.

3.3. *Constrained four criteria region growth*

Region growth is a normal step in target detection. Region growing is a method of combining pixels or sub regions into larger regions based on the prede-
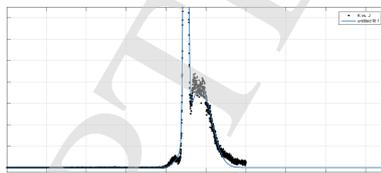

```
General model Gauss2:
       f(x) = a1*exp(-((x-b1)/c1)^2) + a2*exp(-((x-b2)/c2)^2)
Coefficients (with 95% confidence bounds):
       a1 =        3376   (3369, 3382)
       b1 =     3.275e+04   (3.275e+04, 3.275e+04)
       c1 =       29.91   (29.84, 29.98)
       a2 =       376.8   (374.4, 379.1)
       b2 =     3.292e+04   (3.292e+04, 3.293e+04)
       c2 =       199.5   (197.8, 201.2)

Goodness of fit:
  SSE: 1.583e+07
  R-square: 0.9706
  Adjusted R-square: 0.9706
  RMSE: 15.54
```

(a)

(b)

Fig. 4. Fitting results. (a) Curve of Double Gaussian fitting . (b) Result of parameters.

fined growth criteria. The basic processing method starts with a set of seed points to form the growth regions and the predefined attributed the neighborhood pixels are attached to each seed (such as the specified gray level or color). In order to get a suitable region growth result of the specific target detection, this paper proposed a constrained four criteria region growth method. The local maxima are considered to be the seeds to perform the region growth, and the region growth is performed according to the following steps:

Algorithm 2 Four Criteria Region Growth Algorithm

Step 1: traverse the entire image. When seed points are detected, set the eight neighborhood of the seed points as the region of interest. The gray value of the seed point is β and region of interest $R = \{R_1, R_2, R_3, R_4, R_5, R_6, R_7, R_8, R_9\}$, as shown in Fig. 6.a.

Step 2: calculate the maximum of the gray value in the eight neighborhood with the seed point as the center (R_{max}), $R_{max} = \{R_1, R_2, R_3, R_4, R_5, R_6, R_7, R_8\}$.

Step 3: search the four neighborhood (R_{n_1}) of the seed point in turn, $R_{n_1} = \{R_1, R_3, R_5, R_7\}$, as shown in Fig. 6.c. $P \in R_{n_1}$, if $p < R_{max}$ and $\mid p - \beta \mid < \tau_1$, set P as the seed point. If $p = R_{max}$ and $\mid p - \beta \mid < \tau_2$, set P as the seed point and update gray value (β) with the maximum value (R_{max}).

Step 4: search the seed point (R_{n_2}) in the eight domain except four points in the four neighborhood, as shown in Fig .6.b, $R_{n_2} = \{R_2, R_4, R_6, R_8\}$. $P \in R_{n_2}$, if $p < R_{max}$ and $\mid p - \beta \mid < \tau_3$, set P as the seed point. If $p = R_{max}$ and $\mid p - \beta \mid < \tau_4$, set P as the seed point and update gray value (β) with the maximum value (R_{max}).

Step 5: repeat step 2, step 3 and step 4 until all of the seed points are processed. Where $\tau_1 = 30, \tau_2 = 35, \tau_3 = 20, \tau_4 = 25$.

(a)
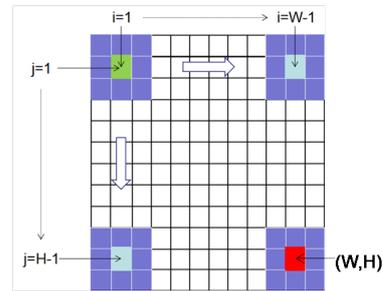
(b)

Fig. 5. (a) 3×3 template window. (b) The way of traversing the entire image.

10   *Yanfeng Wu,Haijiang Sun and Peixun Liu*

3.4. *Confidence measure of candidate targets*

For LSS-Target detection, it is expected to have a high detection rate and low false
alarm rate. However, algorithm mentioned above can remove large areas of complex
background clutter, there are still many edge areas and false targets that cannot
be removed. In this paper, confidence measure is introduced to achieve the target
detection.

Amplified LSS-Target is shown in Fig. 7, the area around the target is approximately the circular. The gray value of the target in the image increases first and
decreases later, as shown in the Fig. 8. Pixels change around the target and all sides
have a gradient, as shown in the Fig. 9.

The confidence $C(A_i)$ takes the form

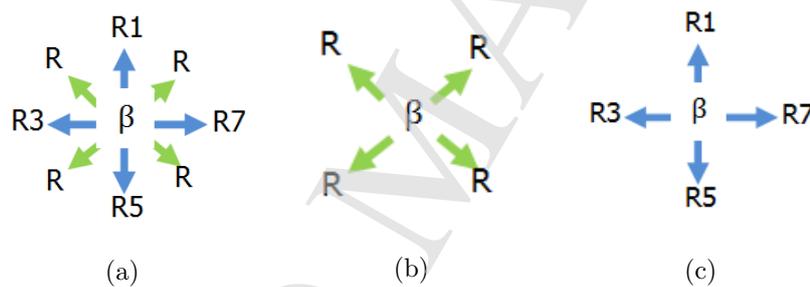$$C(A_i) = C_1(A_i) \times C_2(A_i) \times C_3(A_i) \times C_4(A_i) \times C_5(A_i) \times C_6(A_i) \qquad (3.12)$$

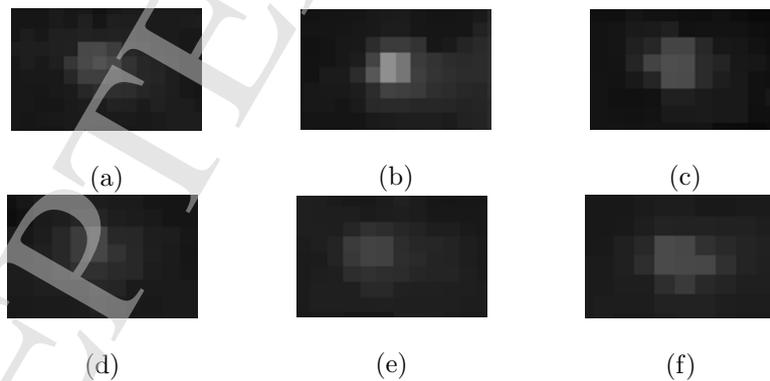Fig. 6. Growth method. (a)Eight neighborhood. (b) Diagonal neighborhood. (c)Four neighborhood.

Fig. 7. Amplified target.

A Novel Fast Detection Method of Infrared LSS-Target in Complex Urban Background   11

where C_1 shows the weight confidence

$$C_1(A_i) = \begin{cases} 0, & if \ w < \gamma_1 \\ 1, & if \ w \geq \gamma_1 \end{cases} \tag{3.13}$$

where w is the weight of candidate targets, C_2 shows the height confidence

$$C_2(A_i) = \begin{cases} 0, & if \ h < \gamma_2 \\ 1, & if \ h \geq \gamma_2 \end{cases} \tag{3.14}$$

where h is the height of candidate targets, C_3 shows the contour length confidence

$$C_3(A_i) = \begin{cases} 0, & if \ L < \gamma_3 \\ 1, & if \ L \geq \gamma_3 \end{cases} \tag{3.15}$$

(a)   (b)   (c)
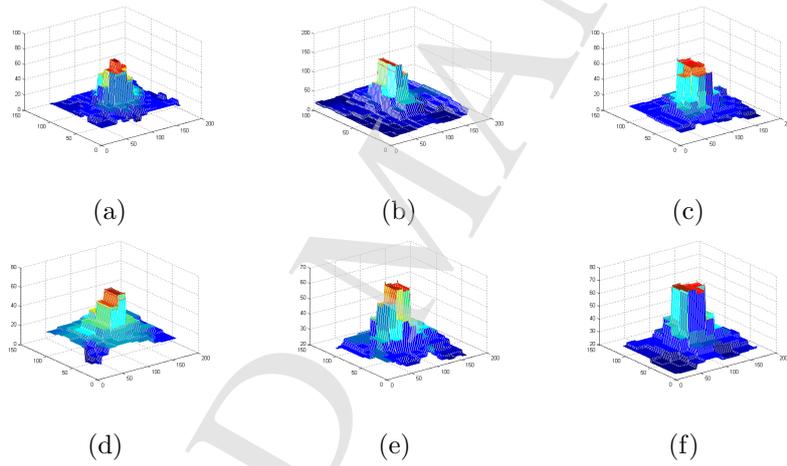
(d)   (e)   (f)

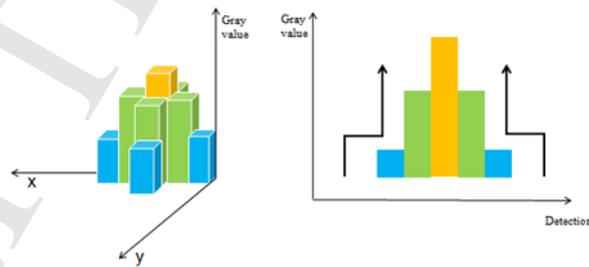Fig. 8. 3D-mesh view of the amplified target.

Fig. 9. Sketch map of gradient variety.

12   *Yanfeng Wu,Haijiang Sun and Peixun Liu*

where L is the contour length of candidate targets, C_4 shows the area confidence

$$C_4(A_i) = \begin{cases} 0, & if \ S < \gamma_4 \\ 1, & if \ S \geq \gamma_4 \end{cases} \quad (3.16)$$

where S is the area of candidate targets, C_5 shows the curvature confidence

$$C_5(A_i) = \frac{\mu_R}{\sigma_R} \quad (3.17)$$

$$\mu_R = \frac{1}{k} \sum_{k=0}^{k-1} ||(x_k, y_k) - (\overline{x}, \overline{y})|| \quad (3.18)$$

$$\sigma_R = \frac{1}{k} \sum_{k=0}^{k-1} [||(x_k, y_k) - (\overline{x}, \overline{y})|| - \mu_R]^2 \quad (3.19)$$

$$\overline{x} = \frac{1}{S} \sum_{(x,y) \in R} x, \ \overline{y} = \frac{1}{S} \sum_{(x,y) \in R} y, \ S = \sum_{(x,y) \in R} 1 \quad (3.20)$$

where μ_R is the average distance from the center of the candidate region to the boundary of the candidate region. σ_R is the mean square deviation from the center of the candidate region to the boundary of the candidate region. Curvature confidence is monotonically increasing and approaches infinity, which is unaffected by regional translation, rotation and scale transformation. where C_6 shows the intensity confidence

$$C_6(A_i) = \frac{1}{1 - e^{-\lambda_1(\mu_A - \mu_{A_i})}} \quad (3.21)$$

where μ_A is the mean gray value of image, μ_{A_i} is the mean gray value of candidate target. The intensity confidence of LSS-Target is close to 1. $\gamma_1 = \gamma_2 = 5, \gamma_3 = 16, \gamma_4 = 3$ in this case.

4. Experimental Results and Analysis

In this experiment, we use an infrared camera to capture the .avi video file with LSS-Target and urban area. The whole image frames number is 1000 and the pixels of the frame is 640×512. The real target is 3km away from the imaging system. The experiments were conducted on Microsoft Visual Studio 2010 software with a 3.2GHZ Intel processor.

The original image shown in Fig. 10. Fig. 11 gives the detection results for the infrared image by using the histogram statistic and the maximum likelihood estimation. We can note that the fusion method can extract the target and the urban area clearly.

Fig. 12 has presented the results of the local maxima and the constrained four criteria region growth, We can see from Fig. 12 that the large areas of urban background clutter is removed successfully.

A Novel Fast Detection Method of Infrared LSS-Target in Complex Urban Background   13

Fig. 13 shows the result of confidence measure, which can eliminate the false targets and detect the real target among candidate targets.

After observing the effect of algorithms proposed in this paper, we calculate the detection accuracy. Experiments demonstrate that the accuracy of the algorithm is up to 95.6%.

There are 64 frames in which the targets cannot be detected, for the difference of gray value between the target and the background are too small to segment. The average number of the false alarms per frame is 0.36.

Table 1. Statistical results of small target detection.

Algorithm	Total Frames	Correct number	False alarm rate
This paper	100	93	14%
Vibe	100	61	46%
Three fame difference	100	46	7%

Table 2. The average time used by the small target detection.

Algorithm	Total Frames	Second per frame (s)	Total time (s)
This paper	100	0.0857243	8.57243
Vibe	100	3.5663	35.663
Three fame difference	100	0.0366987	3.66987

Fig. 10. The original 16-bit image.

To prove the advantages of the algorithm proposed in this paper, ViBe (Visual Background Extractor) and Three Fame Difference method is used to detect the same 100 frames. Time consumption is shown in Table 1, and the comparison is shown in Table 2. Fig. 14 demonstrates the result of Three Fame Difference method.

14   *Yanfeng Wu,Haijiang Sun and Peixun Liu*

Fig. 11. The results of adaptive threshold segmentation.
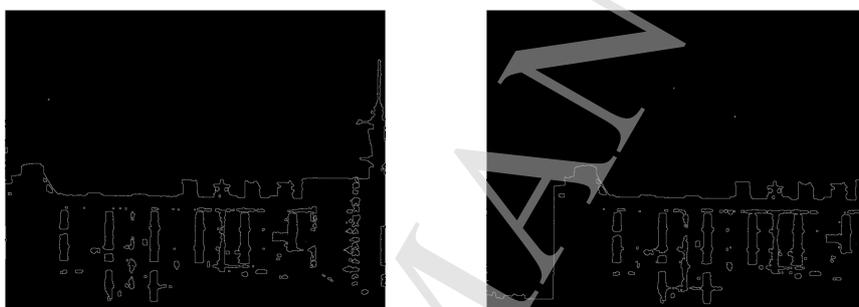

Fig. 12. The results of four criteria region growth.

Fig. 13. Detection results.(Red points are the real target)

Fig. 15 shows the result of Visual Background Extractor. Considering the time consumption and the detection accuracy, the algorithm proposed in this paper has the highest efficiency.

5. Conclusion

Based on the analysis of the feature of LSS-Target, we perform an impactful method in a complex background for LSS-target detection. At first, a novel algorithm based

A Novel Fast Detection Method of Infrared LSS-Target in Complex Urban Background   15

Fig. 14. The results of Visual Background Extractor.

Fig. 15. The results of Three Fame Difference.

on the histogram statistic, the double-Gaussian fitting and the MLE is proposed to extract the ROI. Next, a template is created to detect the local maxima in the IR image, which is regarded as the seeds for the following region growth. A constrained four criteria region growth algorithm is performed to filter out the large areas of clutter. Finally, the confidence measure is proposed to screen out the real target from the candidate targets. This measure can filter out large regions, long regions and edges which cannot be targets. The experimental result shows that the proposed method significantly outperforms the existing methods in time-consuming and detection accuracy and can detect the moving infrared LSS-Target with complex urban background in real time.

References

1. Yu H. and Zhao B., Detection of Small Targets of Low SNR Infrared Images, *LASER and INFRARED.* **34**(1) (2004) 40–42.
2. Fan H., Ni G. and Feng Y., A new algorithm for small and dim target detection of visible image under heavy clutters, *Opto-Electronic Engineering.* **31**(6) (2004) 48–51.
3. B. Babenko,M.H. Yang and S. Belongie, Robust Object Tracking with Online Multiple Instance Learning, *IEEE Computer Society.* **33**(8) (2011) 1619–1632.
4. Tae-Wuk Bae, Small target detection using bilateral filter and temporal cross product in infrared images, *Infrared Physics and Technology.* **54** (2011) 403–411.

16   *Yanfeng Wu,Haijiang Sun and Peixun Liu*

5. I.S.Reed and R.M.Gagliardi, Optical moving target detection with 3-D matched filtering, *IEEE Transactions on Aerospace and Electronic Systems.* **24**(4) (1998) 327–336.
6. X.M. Shen and D. Li, Game theory approach to discrete H1filter design[J]*IEEE Transactions on Signal Processing.* **45**(4) (1997) 1092–1095.
7. V. Caselles, R. Kimmel and G. Sapiro, Geodesic active contours, *International Journal of Computer Vision.* **22**(1) (1997) 61–79.
8. T.F. Chan and L.A. Vese, Active contours without edges, *IEEE Transactions on Image Processing.* **10**(2) (2001) 266–277.
9. Olivier Barnich and Marc Van Droogenbroeck, VIBE: A POWERFUL RANDOM TECHNIQUE TO ESTIMATE THE BACKGROUND IN VIDEO SEQUENCES, *IEEE Transactions on Image Processing.* **20**(6) (2011) 1709–1927.
10. H. Nie, Z. Huang, J. Diao, J. Chen, H. Liu and Q. Li, A wiener filter based infrared small target detecting and tracking method, *Intelligent System Design and Engineering Application.* **20**(1) (2010) 184–187.
11. Y.Zhang, X.Wang and B.Qu, Three-Frame Difference Algorithm Research Based on Mathermatical Morphology, *Procedia Engineering.* **29**(4) (2012) 2705–2709.
12. Yantao Wei, XingeYou and He Deng, Small infrared target detection based on image patch ordering, *International Journal of Wavelets, Multiresolution and Information Processing.***14**(02) (2016) 177–182.
13. E. Guariglia, Entropy and Fractal Antennas, *Entropy.***18**(03) (2016) 1–17.
14. E. Guariglia, Spectral Analysis of the Weierstrass-Mandelbrot Function, *Proceeding of the 2nd International Multidisciplinary Conference on Computer and Energy Science.*(07) (2017) 12–14.
15. E. Guariglia, Fractional Derivative of the Riemann Zeta Function, *Fractional Dynamics.* (2015) 357–368.
16. E. Guariglia and S. Silvestrov, A functional equation for the Riemann zeta fractional derivative, *AIP Conference Proceedings 1798.* 020063